Analysis on Multiple Perforated Plate Sound Absorber Made of Coir Fiber

Md. Ayub

Department of Mechanical and Materials Engineering, Universiti Kebangsaan Malaysia, 43600, UKM Bangi, Selangor, Malaysia
Now working with School of Mechanical Engineering, The University of Adelaide, SA 5005, Australia.

Mohammad Hosseini Fouladi

School of Engineering, Taylor's University, 47500, Subang Jaya, Selangor, Malaysia

Masomeh Ghassem

Faculty of Science and Technology, Universiti Kebangsaan Malaysia, 43600, UKM Bangi, Selangor, Malaysia

Mohd Jailani Mohd Nor

Department of Mechanical and Materials Engineering, Universiti Kebangsaan Malaysia, 43600, UKM Bangi, Selangor, Malaysia

Hamidreza Soheili Najafabadi

School of Industrial Engineering, Iran University of Science and Technology, Narmak, Tehran, Iran

Nowshad Amin

Department of Electrical, Electronic and System Engineering, Faculty of Engineering & Built Environment, Universiti Kebangsaan Malaysia, 43600, UKM Bangi, Selangor, Malaysia
Center of Excellence for Research in Engineering Materials (CEREM), College of Engineering, King Saud University, Riyadh 11421, Saudi Arabia

Rozli Zulkifli

Department of Mechanical and Materials Engineering, Universiti Kebangsaan Malaysia, 43600, UKM Bangi, Selangor, Malaysia

(Received 4 May 2013;revised 15 October 2013; accepted 16 October 2013)

Current studies are aiming to improve the sound absorption of coir fiber by implementing combinations of Perforated Plates (PPs) and air gaps. The Atalla and Sgrad model along with Johnson-Allard model and Acoustic Transmission Analysis (ATA) approach are used to estimate the absorption coefficient of the combination. Measurements are conducted in impedance tube to validate the analytical results. Outcomes show that the absorption coefficient of the panel is governed by the porosities of the implemented PPs. Reduction in the porosity of the face PP causes the incident sound to reflect back whereas higher porosity encourages the sound to enter and be absorbed gradually in the inner compartments. For the case of multilayer panels with two PPs, the best result is obtained when the inner PP has low porosity and is backed with an air gap. Absorption in high and low frequency bands are enhanced by having highly porous material and a thick layer of air gap in front of and behind the inner PP, respectively. This study shows that the high-frequency absorption is enhanced further in panels that include three PP layers. The study suggests fabricating panels containing two or three PPs with gradual reduction of porosity from the face PP to the inner ones, while the inner most PP has low porosity and is backed with air gap.

1. INTRODUCTION

In previous studies on acoustic characteristics of coir fiber,[1–3] it is shown that the absorption coefficient can be improved by using different techniques such as implementation of air gaps and Perforated Plate (PP). However, the thickness of the panel was found to be too large for limited spaces, and the utilization of PPs and air gaps did not improve the low and medium frequency absorption at the same time. For instance, absorption of coir fiber in different arrangements involving single PP and air gap are illustrated in Fig. 1. For 50 mm coir fiber, the absorption is higher than 75% in the medium and high frequency ranges, while addition of a 35 mm air gap promotes the absorption peak towards low frequencies. Addition of a PP with an air gap enhanced the absorption further in the lower region, but at the same time reduced it at mid and high frequency bands. The best result was observed when PP was placed in between the coir fiber and the air gap, but the thickness of 86 mm for the panel was too large for practical applications. Having the upper face of coir fiber without coverings was not suitable for an absorber composed of fibrous material since it could be a potential health risk factor.

Numerous studies were carried out to improve the sound ab-

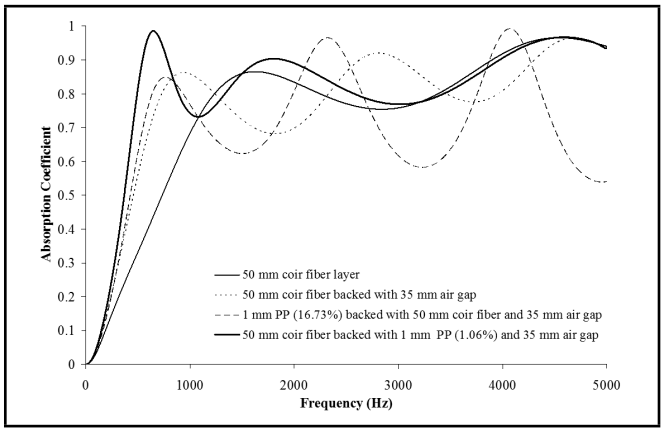

Figure 1. Sound absorption coefficient of the 50 mm coir fiber layer in a different condition.

sorption of a system comprising of single and multiple PPs with and without porous material and air gap. Davern studied multilayer sound absorbers consisting of a perforated facing backed with porous material.[4] Results show that the acoustic impedance and absorption is a function of the porosity of facing and the density of backing material. Dunn and Davern studied the acoustic impedance of multilayer absorbers using Delany-Bazley analytical method.[5,6] They suggested that the multilayer absorber should be chosen in the way that the outermost porous layer encourages the incident sound to enter the composite structure. The inner porous layer attenuated the sound energy and prevented the sound from recombining.[7] Lee and Swenson also showed that the multilayer absorber assembly with two layers of PP backed with air spaces provided better absorption than a single layer.[8] It was reported that the multilayer absorber composed of PP and porous material had better absorption than that of PP and air gap at both low and high frequencies. The sound absorption of the porous layer was also better than that of an air gap with the same thickness.[9] In another study it was evidenced that acoustic resonance frequencies of the multilayer assembly were more broadband than those of their individual compartments. Multilayer absorber composed of porous material may distinctly promote the sound absorption and shift the resonance frequencies towards lower frequency bands.[7]

Chen *et al.* chose four surface shapes of commercially available porous materials, i.e., triangle, semicircle, convex rectangle and plate shapes for analysis over a 1200 Hz band. The fibrous material with triangle, semicircle, or convex shapes had better sound absorption than those with a plate shape.[10] In their further work on multilayer absorbers with different inner structures, they showed that the inner structures influenced the sound absorption at some frequency bands significantly.[11] The quantity of the porous material in front of the outmost layer of PP controlled the absorption at high frequencies. More porous material in front of and behind the PP promoted the absorption at higher and lower frequency bands, respectively. Lee and Kwon proved that the number of PP and arrangement of panels and air spaces have a significant effect on absorption characteristic.[12] The number of PPs could increase the absorption peak, while the arrangement of PPs with a gradual increase in porosity could widen the absorption frequency band. This study investigates the effects of arrangements and the porosity of multiple PPs on the sound absorption of coir fiber, and recommendations are made on the design of efficient panels.

2. METHODOLOGY

Acoustic impedance of coir fiber was predicted by the Johnson-Allard equivalent fluid model as the solid structure of the coir fiber was considered motionless.[13] Surface acoustic impedance of the PP was obtained by the Atalla and Sgard model.[14] The acoustic-transmission approach (ATA) approach was used to estimate the surface impedance of consecutive layers.[7] Finally, different combinations of multilayer structures with multiple PP, coir fiber, and air gap were analyzed by means of these calculation procedures.

2.1. The Johnson-Allard "Equivalent-Fluid" Model

According to the Johnson-Allard Model, the equation for effective density and bulk modulus of the rigid framed porous material is expressed by Eqs. (1)–(4).[13,15] Equation of the Effective density:

$$\rho(\omega) = \rho_0 \alpha_\infty \left(1 + \frac{\sigma\phi}{i\alpha_\infty \rho_0 \omega} G_J(\omega)\right) \tag{1}$$

with

$$G_J(\omega) = \left(1 + \frac{4i\alpha_\infty^2 \eta \rho_0 \omega}{\sigma^2 \Lambda^2 \phi^2}\right)^{\frac{1}{2}}. \tag{2}$$

Equation of the Bulk Modulus:

$$K(\omega) = \frac{\gamma P_0}{\left[\gamma - (\gamma - 1)\left[1 + \frac{8\eta}{i\Lambda'^2 \rho_0 Pr\omega} G'_J(Pr\omega)\right]^{-1}\right]} \tag{3}$$

with

$$G'_J(\omega) = \left(1 + \frac{i\rho_0 \Lambda'^2 Pr\omega}{16\eta}\right)^{\frac{1}{2}}; \tag{4}$$

where ρ_0 is the density of the air, α_∞, σ and ϕ are the tortuosity, flow resistivity and the porosity of porous material, respectively; ω is the angular frequency, f the frequency of sound, i is an imaginary number, Λ and Λ' are the viscous and thermal characteristics length of the porous material, η the viscosity of the air, γ the specific heat ratio of the air, P_0 the atmospheric pressure, and Pr is the Prandtl number.

2.2. Atalla and Sgard Model for PP Modeling

Atalla and Sgard modeled PP as an equivalent fluid following the Johnson-Allard approach with an equivalent tortuosity.[14] In the case of perforated panel backed by a cavity, total input impedance of the perforated-air layer combination is expressed as

$$Z = \left(\frac{2d}{r} + 4\frac{\varepsilon_e}{r}\right)\frac{R_s}{\phi_p} + \frac{1}{\phi_p}(2\varepsilon_e + d)j\omega\rho_0 + Z_B.^{3,14} \tag{5}$$

In the case of the perforated plate in contact with a rigid frame porous layer, the surface impedance is given by the following Equation:

$$Z = \left[\varepsilon_e\left(1 + \Re(\tilde{\alpha}_p)\right) + d\right]\frac{j\omega\rho_0}{\phi_p} + \frac{Z_B}{\phi}; \tag{6}$$

where, d is the thickness of the PP layer, r is the radius of perforation, $R_s = \frac{1}{2}\sqrt{2\eta\omega\rho_0}$ denotes the surface resistance, $\phi_p = \frac{\pi r^2}{b^2}$ is the perforation ratio and is the hole pitch of the

perforation. Z_B is the surface impedance of back coir fiber layer or air gap, and ϕ is the porosity of backed porous material.

In the above equations, ε_e represents a correction length and $\tilde{\alpha}_p$ is the dynamic tortuosity of the porous material, which can be estimated as

$$\varepsilon_e = 0.48\sqrt{\pi r^2}(1 - 1.14\sqrt{\phi_p}); \phi_p < 0.4;^{3,14} \quad (7)$$

$$Re(\tilde{\alpha_p}) = \alpha_\infty \left(1 + \frac{\sqrt{\frac{2\eta}{\rho_0 \omega}}}{\Lambda}\right); \quad (8)$$

where α_∞ is the static tortuosity, and Λ is the viscous characteristic length regarding the porous material. However, if PP is placed between two layers of porous material, the surface impedance is estimated as,

$$Z = [\varepsilon_e(Re(\tilde{\alpha}_{p1}) + Re(\tilde{\alpha}_{p2})) + d]\frac{j\omega\rho_0}{\phi_p} + \frac{Z_B}{\phi}; \quad (9)$$

where, $\tilde{\alpha}_{p1}$ and $\tilde{\alpha}_{p2}$ are the dynamic tortuosity of the face and back porous layer, which is evaluated using Eq. (8) based on the material, and ϕ is the porosity of the porous layer backed by PP.[14]

The ATA method was applied, accompanied by the Atalla and Sgard model to obtain surface acoustic impedance of various consecutives layers together.[7,14] Using the ATA technique, the surface acoustic impedance Γ_j of the jth layer is represented by Eq. (10),

$$\Gamma_j = Z_j \frac{Z_r \cosh(\gamma_j t_j) + Z_j \sinh(\gamma_j t_j)}{Z_r \sinh(\gamma_j t_j) + Z_j \cosh(\gamma_j t_j)}; \quad (10)$$

where Z_j and γ_j are characteristics of the impedance and complex wave propagation constant of the jth layer, and Z_r is the surface acoustic impedance of the back layer.

2.3. Experimental Measurements in Impedance Tube

Experiments were conducted in the impedance tube according to the ISO 10534-2 standard to validate the analytical analysis.[16] The measurement system included two impedance tubes with diameters of 28 and 100 mm each containing two $\frac{1}{4}$" microphones type GRAS-40BP, plane wave source, dual channel Symphonie (01 dB model) real time data acquisition unit and 01 dB software package. Calibrator type GRAS-42AB was used for microphone sensitivity calibration at 114 dB and 1 KHz frequency. Microphones in any of the impedance tubes were calibrated relative to each other using the standard switching technique. Measurements were carried out with 3 Hz frequency resolution and a duration of 10 s. Coir fiber was obtained in the form of large rectangular sheets and then cut into suitable circular shapes and mounted in the impedance tubes. PPs were made of aluminum alloy T6061 and fabricated by a numerically controlled semi-auto machine.

2.4. Flow Resistivity Measurements

The AMTEC C522 air flow resistivity test system was used in compliance with the ASTM C522 standard as 'Test method for Airflow Resistance of Acoustical Material'.[17] Equipment comprises of a sample holder, a vacuum pump, and a data acquisition unit including the C522 software package. The airflow rate and differential pressure ranges between 0 to 15 lpm and 0 to 294.1 Pa, respectively, according to the standard. Measurements were set up for four flow point 1 to 4 lpm with three sequential repeated tests for the same sample to get an average flow resistivity value.

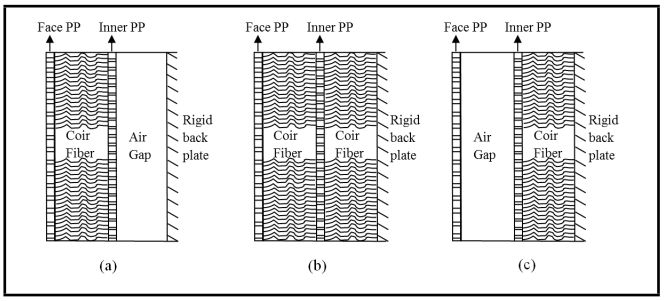

Figure 2. Schematics of two PPs system in three different assemblies. (a) Face PP backed with coir fiber and inner PP backed with air gap; (b) Both PPs backed with coir fiber; (c) Face PP backed with air gap and inner PP backed with coir fiber.

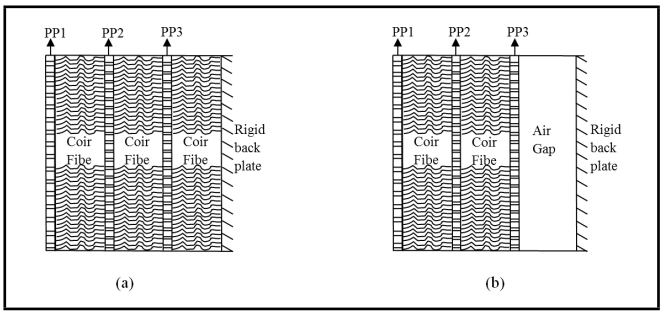

Figure 3. Schematics of the three PP systems in two different assemblies. (a) Three PPs each backed with an coir fiber; (b) Both outermost and inner PP backed with coir fiber; and innermost PP backed with an air gap.

2.5. Combinations of the Layers

Three combinations were studied for the case of a panel including two PPs as shown in Figs. 2(a)-2(c). Figure 2(a) shows that the face PP was backed with coir fiber while the air gap was behind the inner PP. Figure 2(b) was the case that both PPs were backed with coir fiber. The combination in Fig. 2(c) is similar to Fig. 2(a) but the position of coir fiber and air gap layers are swapped. Figures 3(a) and Fig. 3(b) present the two combinations that were studied for the case of having three PPs in the panel. All the PPs are backed with coir fiber in Fig. 3(a) while for the combination Fig. 3(b), the inner most PP is backed with air gap. Combinations shown in Fig. 2 and Fig. 3 are investigated throughout the paper and recommendations are made to enhance the sound absorption for both the two and three PPs systems.

3. RESULTS AND OBSERVATIONS

The rigid frame Johnson-Allard equivalent fluid model was employed to estimate the characteristics of the impedance of coir fiber with some modifications in the geometrical parameters of fiber.[13] The real diameter of fibers mixed with binder in the porous material was calculated as[3]

$$d_{mix} = d_{fiber} + (d_{fiber}\phi); \quad (11)$$

where d_{mix} and d_{fiber} are the diameter of fiber after and before mixing with binder, respectively. The new unit volume of the material was wholly occupied by the fiber-binder mixture, and

the total length per unit volume l_{mix} developed as[3]

$$l_{mix} = \frac{1}{\pi r_{mix}^2}; \tag{12}$$

where $r_{mix} = \frac{d_{mix}}{2}$ and the viscous characteristic length was calculated as below:

$$\Lambda_{mix} = \frac{1}{2\pi r_{mix} l_{mix} \phi}. \tag{13}$$

The flow resistivity of the fiber was estimated from the empirical equation (14) as having the bulk density of the sample and the diameter of the fiber,[3,18]

$$\sigma = 490 \frac{\rho_{bulk}^{1.61}}{d_{mix}}. \tag{14}$$

The flow resistivity was measured experimentally for 20 and 50 mm samples and compared with the numerical values as shown in Table 1. It proved that Eq. (14) may be utilized to predict the flow resistivity of coir fiber.

PP was modeled as an equivalent fluid using the Atalla and Sgard model.[14] Acoustic surface impedance of PP backed with coir fiber or air gap was the addition of impedance of PP and the impedance of coir fiber or air gap. Surface impedance of the PP was calculated using Eq. (5) or Eq. (6) based on the PP backing layer (air gap or coir fiber). Characteristics of impedance and propagation constant of coir fiber were calculated using Eqs. (1)-(4) customized by Eqs. (11)-(14). The surface impedance of consecutive layers was calculated using the ATA method as shown in Eq. (10), starting from first layer backed with a rigid wall, and then this impedance was substituted as the back surface impedance for the next layer.

Combinations of Figs. 2(a) and 2(b) were analysed to validate the accuracy of the analytical predictions using the rigid frame model. The measured and analytical absorption coefficient of these combinations are presented in Figs. 4 and Fig. 5 together with the prediction error rate.[19] As shown in Fig. 4, the porosities of PPs were $\phi_{p1} = 13.39$ % ($r = 1.9$ mm and $b = 9$ mm) and $\phi_{p2} = 9$ % ($r = 0.95$ mm and $b5.6$ mm), and the thicknesses of the coir fiber layer and the air gap were 50 and 35 mm, respectively. To calculate the total impedance of combination Fig. 2(a), surface impedance of inner PP backed with 35 mm air gap was estimated using Eq. (5) as PP was backed with air gap. Then, characteristics impedance of 50 mm coir fiber layer was estimated using rigid frame model. ATA approach presented in Eq. (10) was employed to calculate the surface impedance of interaction layer between coir fiber-inner PP, considering the impedance of the inner PP as back surface impedance. Thereafter, surface impedance of the face PP was obtained using Eq. (6) as the face PP backed with porous material. Calculated combined surface impedance of the consecutive arrangement of coir fiber-PP-air gap for combination Fig. 2(a), was the back impedance for PP formulation in Eq. (6). By means of these calculations, the resultant total surface impedance of the panel was derived and the corresponding absorption coefficient was estimated.

Fig. 5 represents the results for combination Fig. 2(b). The porosities of the PPs were $\phi_{p1} = 16.87$ % ($r = 0.95$ and $b = 4.1$ mm) and $\phi_{p2} = 9$ % ($r = 0.95$ and $b = 5.6$ mm). The thicknesses of coir fiber layers in the outer layer and inner compartments were 50 mmand 30 mm, respectively. The calculation procedure to evaluate the total surface impedance of this combination was the same as mentioned for combination

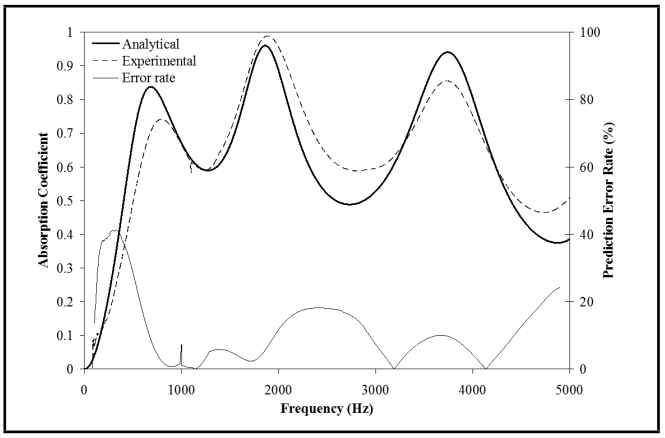

Figure 4. Comparison between the measured and calculated absorption coefficient of combination Fig. 2(a). One (1) mm face PP ($\phi_{p1} = 13.39$ % with $r = 1.9$ and $b = 9$ mm) backed with 50 mm coir fiber and 1 mm inner PP $\phi_{p2} = 9$ % with $r = 0.95$ and $b = 5.6$ mm) backed with 35 mm air gap.

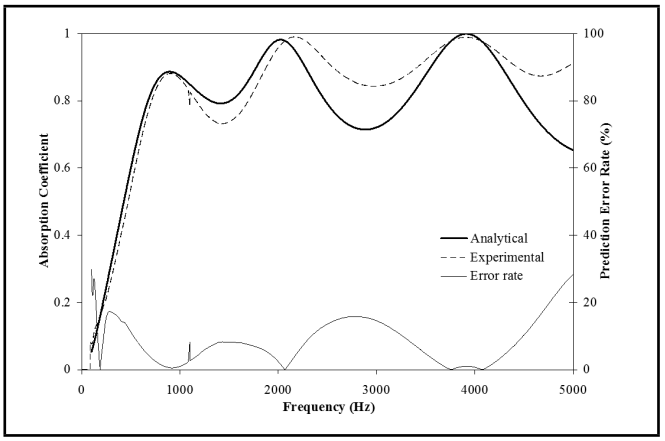

Figure 5. The sound absorption coefficient of combination Fig. 2(b). One (1) mm face PP ($\phi_{p1} = 16.87$ % with $r = 0.95$ and $b = 4.1$ mm) backed with 50 mm of coir fiber and 1 mm inner PP ($\phi_{p2} = 9$ % with $r = 0.95$ and $b = 5.6$ mm) backed with 30 mm of coir fiber.

Fig. 2(a) except the inner air gap layer was replaced by another fiber layer. To estimate the surface impedance of the inner PP for this combination, Eq. (9) was employed instead of Eq. (6), since the PP was located in between two coir fiber layers. As illustrated in Figs. 4 and Fig. 5, the results of the present rigid frame model were in agreement with the experimental results. Anomalies in the results were due to imperfections in the PP fabrication that caused the uneven tapering and non-uniform perforation radius as addressed in authors previous work.[3] The comparison of the measured absorption coefficients and those predicted by the rigid frame method using the mean error rate showed discrepancies lower than 20% for both cases in the frequency range 0.2–4.2 kHz. Results proved that the rigid frame model could be used successfully as an analytical tool for other multilayer panels instead of the complex Allard transfer function (TF) method.[3,13]

Results for the analytical and measured absorption coefficients of the three PPs combinations Figs. 3(a) and 3(b) are presented in Fig. 6 and Fig. 7, respectively along with the prediction error rate. They show that the present rigid frame model was once again in agreement with the experimental results. However, the position of the second and third absorption peaks were not properly estimated with this analytical method. Irregularities may be due to the improper alignment of the layers and inaccurate measurement of the thickness of porous

Table 1. Comparison between the estimated and experimentally measured flow resistivity for the two samples of industrial prepared coir fiber.

Thickness (mm)	Mass of the sample for 100 mm diameter (gm)	Flow Resistivity(Nsm^{-4}) Estimated using Eq. (14)	Flow Resistivity Nsm^{-4} By measurement
20	15.50	1680	1618
50	34.13	1359	1395

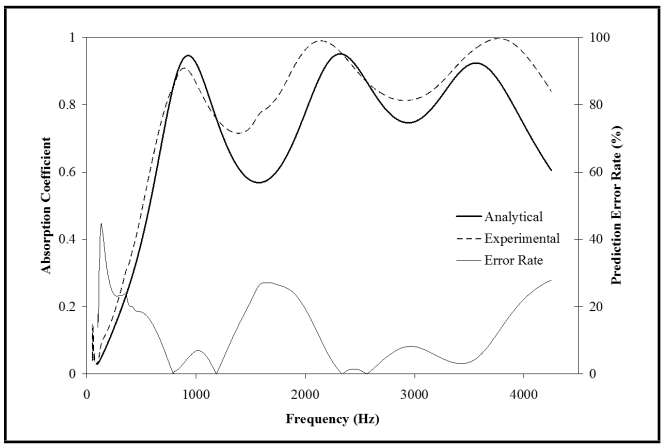

Figure 6. Sound absorption coefficient of combination Fig. 3(a) for the three PP combination. Porosities of PPs are ($\phi_{p1} = 17.32$ %, $\phi_{p2} = 8.89$ % and $\phi_{p3} = 7.56$ %). Thickness of each compartment is 20 mm. Total thickness of the panel is 63 mm.

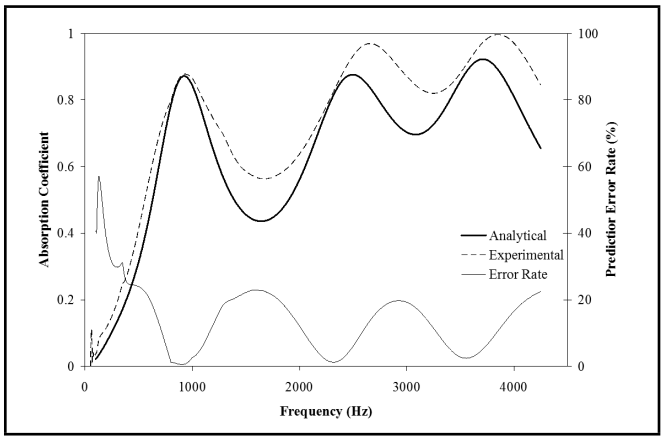

Figure 7. Sound absorption coefficient of combination Fig. 3(b) for three PP combinations. Porosities of PPs are ($\phi_{p1} = 17.32$ %, $\phi_{p2} = 8.89$ % and $\phi_{p1} = 7.56$ %). The thickness of each compartment is 20 mm. The total thickness of the panel is 63 mm.

layer. Discrepancies between the experimental and analytical results were increased by increasing the number of layers. Lee and Chen explained that the inevitable disagreement between the calculated surface acoustic impedance of the PP and the acoustic characteristics of the practical PP might cause the errors.

It is suggested to accept the rigid frame model as a reliable analytical procedure for multilayer assembly. Therefore, various combinations of multilayer assembly were analytically studied using the rigid frame method to explore the effects of different factors on sound absorption of multiple PP absorbers.

3.1. Two PP Sound Absorber

In order to evaluate the acoustical characteristics of multiple PP absorbers, the assemblies of two layers of PPs backed with coir fiber or air gaps were first analysed. This work was mainly focused on the improvement of coir fiber absorption coefficient by obtaining wideband absorption and at the same time maintaining a reasonable panel thickness. A fixed panel thickness, at least lower than the cases mentioned in Fig. 1, was chosen

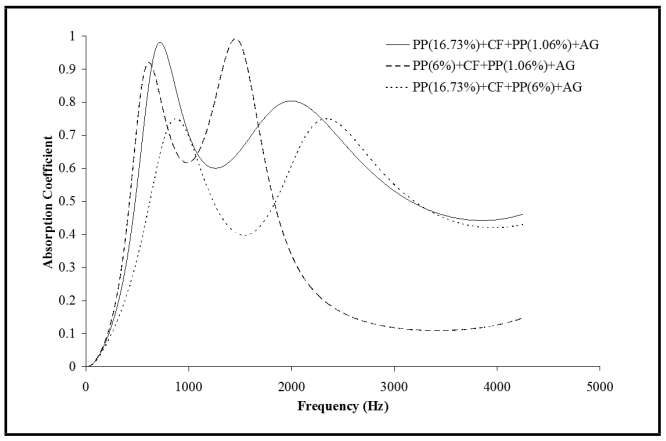

Figure 8. Sound absorption coefficient of combination Fig. 2(a) for three different combinations of porosities.

to demonstrate the characteristics. Hence, the total thicknesses of the assemblies are varied within the range of 60–63 mm for further analyses.

3.1.1. Effect of PP Porosity

The total thickness of the panel shown in Fig. 2(a) was taken as 62 mm, PPs had thickness of 1 mm, and the coir fiber and air gap layers were 30 mm each. The absorption plots of this combination in three different arrangements of porosities are shown in Fig. 8. Notation CF is for Coir fiber, AG is for air gap, and PP is for perforated plate. Thickness of each compartment is mentioned in the parentheses. The combination of porosities were $\phi_{p1} = 16.73$ % and $\phi_{p2} = 1.06$ %, $\phi_{p1} = 6$ % and $\phi_{p2} = 1.06$ %, and $\phi_{p1} = 16.73$ % and $\phi_{p2} = 6$ %. It was observed that the porosity of PP had a significant effect on absorption performance of the multilayer PP system. Absorption of the panel with two PPs was maximized at resonance frequencies which were considerably affected by the porosities of the two PPs. For the cases with porosities $\phi_{p1} = 16.73$ % and $\phi_{p2} = 1.06$ %, it was observed that varying the porosity of the face PP changed the absorption coefficient. Position of second resonance peak and the sound absorption of the first peak were almost similar for both cases as the porosity of inner PP remained constant. It was understood that the resonance frequency and the absorption were governed by porosity of the inner PP and the face PP, respectively.

Furthermore, the total absorption of the panel also depends on the porosity of both PPs. As shown in Fig. 8, the sound absorption for the case with porosities $\phi_{p1} = 16.73$ %, $\phi_{p2} = 1.06$ % was generally broader and higher than that of the case with porosities $\phi_{p1} = 6$ %, $\phi_{p2} = 1.06$ %, except for the relatively lower absorption in the mid-frequency range and very low absorption in the high-frequency range for both cases. The difference between these two cases was the porosity of the face PP. For the latter case, low porosity ($\phi_{p2} = 6$ %) of the face PP promoted the second resonance peak towards lower frequency and caused higher absorption in the low- and mid-frequency ranges but almost no absorption was observed in high frequency region. On the other hand, higher porosity of the face PP ($\phi_{p1} = 16.73$ %) shifted the second resonance peak towards higher frequency and induced compar-

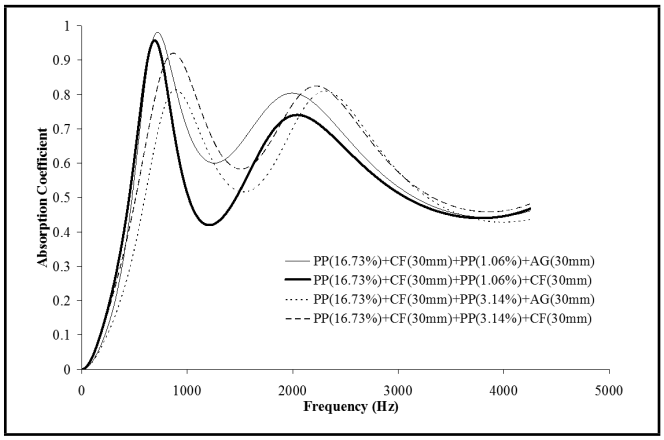

Figure 9. Sound absorption coefficient of combination Fig. 2(a) and Fig.2(b) for two different porosities.

atively wider absorption than the case of the low porosity of face PP ($\phi_{p1} = 6$ %). These differences could be attributed to having resonance frequency in the multilayer absorber addressed by the previous researchers.[7,12] A drop in the porosity of the face PP caused the incident sound to reflect from the PP surface, whereas higher porosity allowed the sound to enter in the inner structure gradually and be absorbed in the inner compartment. The high porosity of the inner PP (ϕ_{p2}) showed the reduction of absorption for both peaks. As it was shown for the case with the porosities $\phi_{p1} = 16.73$ % and $\phi_{p2} = 6$ %, when the porosity of the inner PP was increased (e.g.= $\phi_{p2} = 6$ %), the sound absorption decreased. It was noticed that the sound absorption for the case with porosities $\phi_{p1} = 16.73$ %, $\phi_{p2} = 1.06$ % exhibited the best results among the three conditions. In this case, higher porosity of the face PP promoted the incident sound to enter into the inner structure and then it reached inside the Helmholtz resonator, which contributed to absorb low frequency sound. It was concluded that better absorption could be obtained by providing a larger difference between the two porosities of PPs and maintaining higher porosity of the face PP and lower porosity of the inner PP.

3.1.2. Effect of Accompanied Layer of Porous Materials

It was shown that the porosity of the PP had a significant role in the performance of multiple PP absorbers. This section describes how the extra coir fiber layer influences the absorption of panels including multiple PPs. Interesting results were observed when the inner air gap layer was replaced by another coir fiber layer with same thickness as shown in Fig. 2(b). Figure 9 shows the absorption coefficient for both combinations Figs. 2(a) and 2(b) with two different porosities. Results illustrate that the sound absorptions for the case of $\phi_{p1} = 16.73$ % and $\phi_{p2} = 1.06$ % were higher when the inner PP was backed with an air gap rather than coir fiber. On the contrary, for the case with porosity of $\phi_{p1} = 16.73$ % and $\phi_{p2} = 3.14$ % absorption decreased when inner PP was backed with an air gap. Porosity of the inner PP (ϕ_{p2}) in the latter case was increased to 3.14 % from 1.06 %, which resulted in less absorption for the inner PP backed with an air gap.

In the case with porosities $\phi_{p1} = 16.73$ % and $\phi_{p2} = 1.06$ %, low porosity of the inner PP caused the Helmholtz effect due to the back air gap. This had more effect on the sound absorption of the panel compared to the resistive effect produced by coir fiber. Putting porous material at the back of the inner PP layer with low porosity ϕ_{p2} may induce a certain part of the incident sound to reflect from the inner PP surface. The reflected sound waves can possibly recombine with the incident sound waves to cause a large reduction in the absorption in between the two peaks when the inner PP is backed with coir fiber. Looking at the case with porosities $\phi_{p1} = 16.73$ % and $\phi_{p2} = 3.14$ % and the inner PP backed with coir fiber, high porosity of the inner PP promotes the resistive effect to be more dominant than Helmholtz effect. Therefore, sound absorption was better for the case of porosities $\phi_{p1} = 16.73$ % and $\phi_{p2} = 3.14$ % when the inner PP was backed with coir fiber rather than air gap. Results demonstrated that multilayer assembly containing two PPs give better results when the inner PP has low porosity and is backed with an air gap. Increasing the porosity of inner PP reduced the sound absorption of multilayer structure. Replacing air gap with coir fiber can reduce the absorption if the porosity of PPs is not chosen properly. Outcomes also indicate that the absorption does not only depend on the porosities but is substantially affected by the accompanied layers.

3.1.3. Effect of Different Combination or Arrangement

To reveal the effects of different arrangement, the multilayer absorbers composed of two PP, coir fiber, and/or an air gap were considered as shown in Fig. 2. For combination Fig. 2(a) and Fig.2(b), the thickness of each PP backing layer was kept as 30 mm in all combinations. From the previous analyses, it was found that if the inner PP was backed with coir fiber then the porosity should be low, whereas if the inner PP was backed with an air gap, then the porosity should be less than before, hence have better sound absorption. Therefore, a similar criterion was maintained for all combinations. The sound absorption characteristics of the arrangement for combination Fig. 2(a) and Fig.2(b) were already explained in section 3.1.2. and the absorption plot was displayed in Fig. 9.

Another possible combination for two PP systems was illustrated in Fig. 2(c), where the absorber was composed of a 1 mm face PP backed with a 30 mm air gap and a 1 mm inner PP backed with a 30 mm coir fiber layer. The absorption plot of that combination is exhibited in Fig. 10 with two different arrangement of porosities $\phi_{p1} = 1.06$ %, $\phi_{p2} = 16.73$ % and $\phi_{p1} = 16.73$ %, $\phi_{p2} = 1.06$ %. For combination Fig. 2(c) with the porosities $\phi_{p1} = 1.06$ % and $\phi_{p2} = 1.06$ %, absorption of second resonance peak in mid-frequency was greatly reduced, and the first resonance peak was shifted towards lower frequencies; no considerable absorption was observed at a high frequency. The lower porosity of the face PP caused most of the incident sound to be reflected from the PP surface despite it being near the resonance frequency and thus flattening the second peak. It was of interest to know what happens if the face PP is replaced with higher and inner PP with lower porosity for the same combination Fig. 2(c). Therefore, the absorption graph for the case with porosities $\phi_{p1} = 16.73$ %, $\phi_{p2} = 1.06$ % was also included in Fig. 10. Results reveal that the absorption was reduced and a single resonance peak was observed in low frequency instead of two resonance peaks. With respect to the previous results (section 3.1.1) regarding the resonances in the PP arrangements, peak could be regarded as the resonance induced by the inner PP. Then the combination was acting like a panel with a single PP backed by coir fiber, and the face compartment did not have any effect on the absorption due to the higher porosity of face PP. The higher porosity of the face PP backed by an air gap was behaving like an open air space in

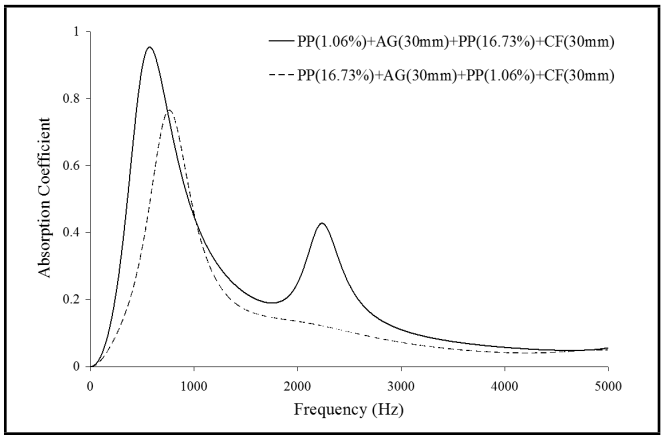

Figure 10. Sound absorption coefficient of the combination Fig. 2(c) for different porosities.

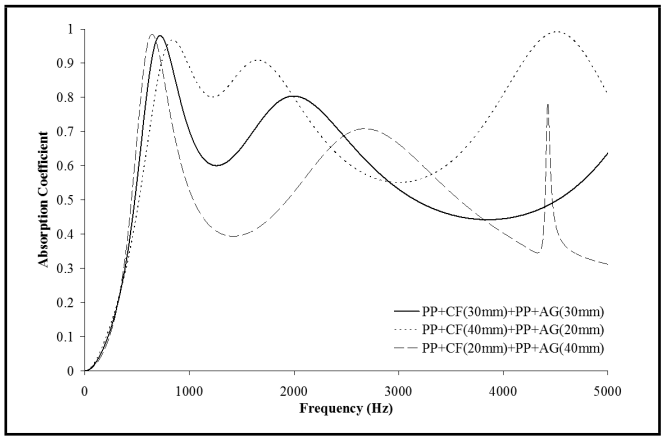

Figure 11. Sound absorption coefficient of the combination Fig. 2(a) with different layer thicknesses. Porosities of PPs are $\phi_{p1} = 16.73\ \%$ and $\phi_{p2} = 1.06\ \%$.

front of the inner PP. Besides, the porosity of the face PP became too large for an air gap to create resonance as well as Helmholtz effect.

Comparing the sound absorption for these three arrangements summarized in Fig. 9 and Fig.10, it was noticed that the combination Fig. 2(a) gave the best result among all three arrangements for the same assembly of porosities and thickness of the panel. Additionally, it could be addressed that filling all compartments with porous layer did not have a considerably favorable effect, rather the inner compartment occupied with an air gap provided better results for low frequency. Therefore, in two PP systems, an air gap should also be included instead of coir fiber. The air gap should be placed in the inner compartment with lower porosity of the inner PP to achieve better results.

3.1.4. Effect of Layer Thickness

The acoustic resonance peak of the multilayer absorber composed of two PPs with coir fiber and an air gap were investigated. It was found that the panel composed of two PPs backed with an coir fiber and air gap, respectively had better absorption than that of both PPs backed with coir fiber layers. Therefore, combination Fig. 2(a) was chosen to explain the effect of layer thickness. Fig. 11 exhibits the absorption coefficient for the assembly in three different combinations of layer thicknesses. Porosities of two PPs were kept constant as $\phi_{p1} = 16.73\ \%$ and $\phi_{p2} = 1.06\ \%$. The absorber composed of two compartments of coir fiber and an air gap was backed by PP, and the layer thickness of each compartment was 30 mm. The layer thickness of each compartment was varied by 10 mm to examine the effect of layer thickness. Absorption in mid frequency was enhanced when the thickness of the first compartment was increased to 40 mm, and that of the second compartment decreased to 20 mm to maintain a total constant thickness. Additionally, both resonance peaks came closer with the change of layer thickness, and thus the absorption band became narrower. When the thickness of the first compartment was decreased to 20 mm and the second compartment increased to 40 mm, a reduction in absorption was observed in the mid-frequency, and both peaks move away from each other to produce a wider absorption bandwidth. A third peak appeared in higher frequency range. The interpretation was that if the thickness of the coir fiber layer was decreased gradually from 40 mm to 20 mm, the second resonance peak moved towards higher frequency bands and the absorption reduced. When the thickness of the air gap was increased from 20 mm to 40 mm, the first resonance peak moved towards lower frequency with an almost similar absorption effect. Another third peak appeared whenever the layer thickness of either compartment (coir fiber or air gap) became 40 mm. These behaviors can also be examined by the comparison of the sound absorption characteristics of each separated individual compartment for that multilayer combination as displayed in Fig. 12 and Fig.13, respectively. The first resonance peak was induced due to the inner compartment (i.e., PP backed with an air gap, and the second peak was induced by the face compartment; the face PP backed with coir fiber). The third narrow peak appeared in high frequency due to the increased layer thickness of either compartment of coir fiber or an air gap. However, as illustrated in Fig. 11, when the thickness of the fiber layer in the face compartment was increased, the third peak became wider than the one provided by the increased inner air gap thickness. Subsequently, low frequency absorption curves remained very similar for inner air gap thickness varying from 20 to 40 mm, despite a slight movement towards lower frequency. Results implied that more porous material in front of the inner PP increased the absorption in high frequency; whereas, addition of a thicker air gap behind the inner PP promoted the resonance peak towards lower frequency. The absorption coefficient in high frequency bands was greatly reduced when two PPs were used. Therefore, to improve high frequency absorption of the multilayer coir fiber absorber, three PP assemblies were also analyzed by the present rigid frame model.

3.2. Three PP Sound Absorber

Two possible arrangements of three PP system were studied as displayed in Fig. 3. Outcomes of three layer PPs backed with coir fiber are shown in Fig. 14. It was shown that increasing the number of PP layers gave better results in sound absorption for the wide frequency region compared to other absorbers despite the drops of absorption in between peaks. Numbers of resonance peaks were increased and induced peaks were the same as the number of PPs. This type of behavior was also addressed by Lee and Kwon.[12] In order to check the effect of each PP layer on the resonance peak in a multilayer structure, the absorption plots of single PP, two PP, and three PP absorbers were also compared. In Fig. 14, the dotted line represents the single PP ($\phi_{p3} = 3.14\ \%$) backed with 20 mm coir fiber. The dashed line exhibits the absorption for the two PP ($\phi_{p2} = 8.7\ \% \wedge \phi_{p3} = 3.14\ \%$) system in which each

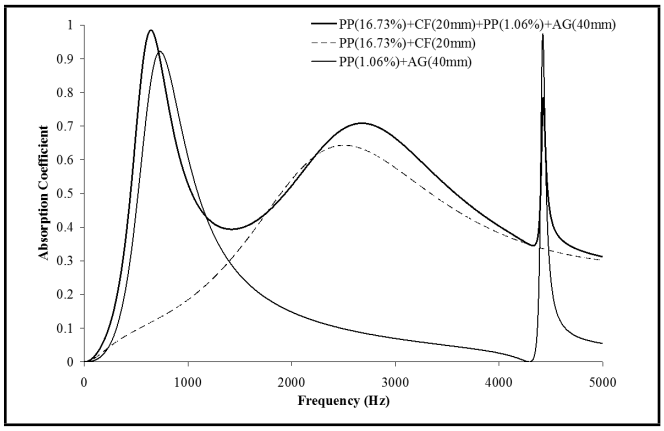

Figure 12. Sound absorption coefficient of combination Fig. 2(a) and that of each separated individual compartment for the layer thickness of 20 mm of coir fiber and a 40 mm air gap.

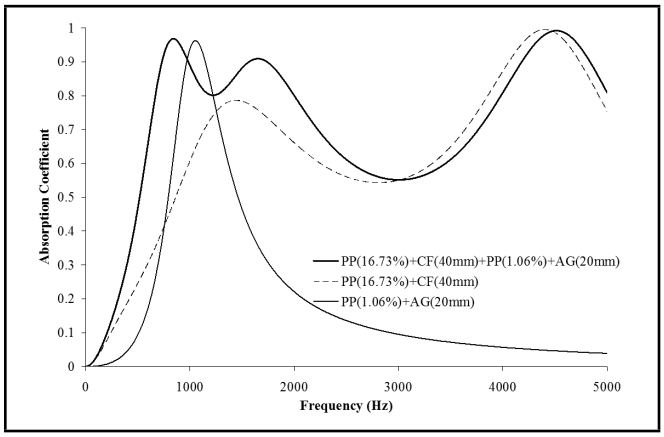

Figure 13. Sound absorption coefficient of combination Fig. 2(a) and that of each separated individual compartment for the layer thickness of 40 mm of coir fiber and a 20 mm air gap.

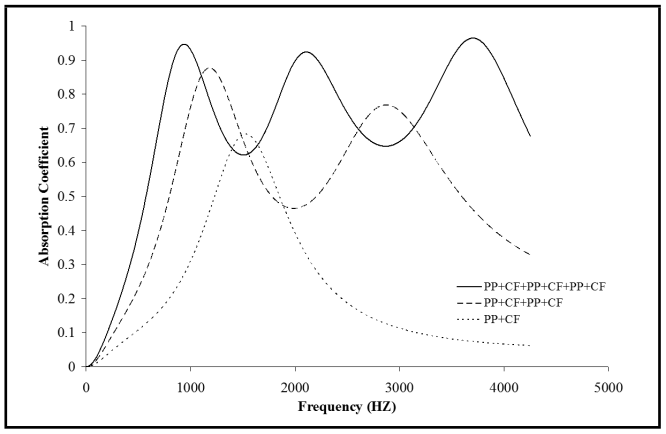

Figure 14. Sound absorption coefficient of a multilayer coir fiber absorber for different numbers of PPs.

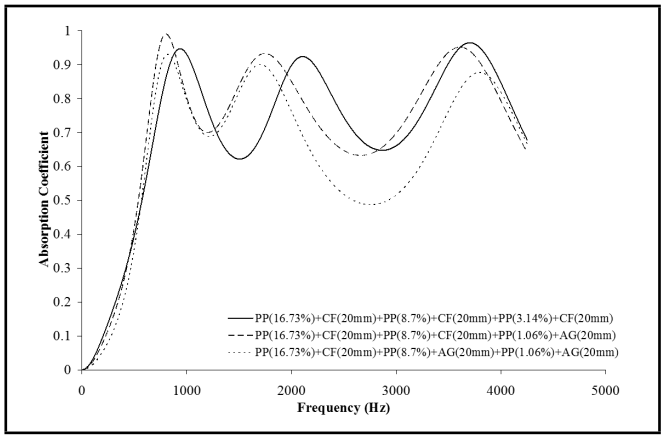

Figure 15. Sound absorption plots of three PP absorbers with a different layer arrangement.

PP is backed with 20 mm of coir fiber. The solid line corresponds to the absorber with three PPs and with porosities $\phi_{p1} = 16.73$ %, $\phi_{p2} = 8.7$ %$\wedge\phi_{p3} = 3.14$ %, and when each PP was backed with 20 mm of coir fiber. The results show that the absorption peak of multilayer PP assembly was governed by each PP layer. The inner most PP layer induced a lower frequency resonance peak, while the inner PP layer controlled the mid-frequency resonance peak and the outermost PP provided high frequency resonance peak. The three layer PP arrangements enhanced the absorption in the overall frequency spectrum. A drawback of the two PP assemblies was improved with the three PP systems (i.e., high frequency absorption was enhanced). Moreover, this configuration demonstrates the significant improvement in the absorption coefficient of the perforated absorber comparing to the same thickness (62 mm) of two PPs systems.

Based on previous findings,[7,12,20] it was understood that arrangement of PPs with a gradual decrease in porosities from the face PP to the inner-most PP should be chosen to obtain wider absorption. However, when the inner-most PP was backed with an air gap, then the porosity of the inner PP should be less than the one provided for the case with coir fiber. As a result, two different assemblies of porosities for PPs were considered. For the case of all PPs backed with coir fiber, the porosities of PPs were $\phi_{p1} = 16.73$ %, $\phi_{p2} = 8.7$ %$\wedge\phi_{p3} = 3.14$ %; and for the case in which the inner most PP was backed with an air gap, the porosities were ($\phi_{p1} = 16.73$ %, $\phi_{p2} = 8.7$ %$\wedge\phi_{p3} = 1$). Fig. 15 describes how the peak and the absorption coefficient of the three-layer PP system is influenced by the arrangement of layers. Comparison of absorption between these two cases showed that the latter case in which the inner PP is backed with an air gap gave better low frequency absorption. These types of behavior were obvious since it was already observed with the two layers PP layer system, as explained previously. The high frequency absorption was reduced when the middle compartment was occupied with an extra layer of air gap for the case $\phi_{p1} = 16.73$ %, $\phi_{p2} = 8.7$ %$\wedge\phi_{p3} = 1$ %, certainly again.

The suggestion is that for a multilayer panel containing two or three PPs, it is better to have at least one inner-most PP with a lower porosity backed by air gap instead of a porous layer to enhance the absorption at a low frequency band. This combination helped to keep the absorption at a reasonable level in mid- and high-frequency regions as well.

3.3. Factors to be Considered during the Design of Multiple PP Absorbers

From the abovementioned analysis, the following recommendations are made for the future design of a multilayer PP sound absorber utilizing coir fiber.

1. Porosity of the PPs is chosen properly to control the absorption of a multiple PP system. Higher porosity of a face PP and lower porosity of an inner PP are important factors to obtain good absorption in the case of two PP system. Similarly, in the case of three PP system, progressive decrease in porosities for a face PP to an inner PP

encourages the sound to enter the inner layer with proper absorption in each compartment.

2. Better sound absorption is obtained in a multiple PP system, if PPs are chosen with large possible differences between their porosities. However, previous recommendation should be maintained (i.e., the porosity of PPs should be decreased progressively). If the inner PP is backed with an air gap, then the porosity of the PP should be less than the case of the inner PP backed with coir fiber to provide better low-frequency absorption.

3. More porous material in front of an inner PP (or behind the face PP) enhances the absorption in high frequency, whereas more porous material at the back layer of the inner PP promotes low frequency absorption. Existence of an air gap behind the inner PP with proper porosity (as mentioned above) may provide better low frequency absorption than that of having porous material behind the inner PP.

4. The number of resonance peaks changes with the number of PPs applied to the system. As a result, PPs can be employed based on the required absorption frequency band. The resonance peak of a multiple PP system is controlled by each PP layer accordingly with their backed compartment. The inner-most PP layer contributes to a lower frequency resonance peak, while the inner PP layer controls mid-frequency resonance peak and the outermost PP provides a high-frequency resonance peak.

5. It is better to have at least one single layer of an air gap in the multiple PP system, instead all the compartments are occupied with porous material. It improves the low frequency absorption better than that of all the compartments filled with porous material. However, the air gap layer should be in the innermost layer with very low porosity of the innermost PP.

4. CONCLUSION

The rigid frame model of coir fiber together with the ATA approach and the Atalla and Sgard model were applied to estimate the absorption coefficient of multiple PP systems composed of coir fiber and an air gap. Various combinations of multilayer assembly with multiple PP, coir fibers and air gap were analyzed by using the model. Results showed that proper design of the panel elements enhanced the absorption coefficient in a wider frequency range. Comparisons showed that using multiple PPs helps to reduce the thickness of the panel while preserving wideband absorption. It is also proved that coir fiber is a novel source of porous material for sound absorption applications.

REFERENCES

[1] Hosseini Fouladi, M., Mohd. Nor, M. J., Ayub, M., Ghassem, M. Enhancement of coir fiber normal incidence sound absorption coefficient, *J. of Comp. Acoust.*, **20**(1), 125003.1–125003.15, (2012).

[2] Hosseini Fouladi, M., Ayub, M., Mohd. Nor, M. J. Analysis of coir fiber acoustical characteristics, *Appl. Acoust.*, **72**(1), 35–42, (2011).

[3] Hosseini Fouladi, M., Nor, M. J. M., Ayub, M. and Leman, Z. A. Utilization of coir fiber in multilayer acoustic absorption panel, *Appl. Acoust.*, **71**(3), 241–249, (2010).

[4] Davern, W. A. Perforated facings backed with porous materials as sound absorbers - an experimental study, *Appl. Acoust.*, **10**(2), 85–112, (1977).

[5] Dunn, I. P. and Davern, W. A. Calculation of acoustic impedance of multi-layer absorbers, *Appl. Acoust.*, **19**(5), 321–334, (1986).

[6] Delany, M. E. and Bazley, E. N. Acoustical properties of fibrous absorbent material, *Appl. Acoust.*, **3**(2), 105–116, (1970).

[7] Lee, F. C. and Chen, W. H. Acoustic transmission analysis of multi-layer absorbers, *J. Sound Vib.*, **248**(4), 621–634, (2001).

[8] Lee, J. and Swenson, G. W. Compact sound absorbers for low frequencies, *Noise Cont. Eng. J.*, **38**(3), 109–117, (1992).

[9] Congyun, Z. and Qibai, H. A method for calculating the absorption coefficient of a multi-layer absorbent using the electro-acoustic analogy, *Appl. Acoust.*, **66**(7), 879–887, (2005).

[10] Chen, W. H., Lee, F. C., Chiang, D. M. On the acoustic absorption of porous materials with different surface shapes and perforated plates, *J. Sound Vib.*, **237**(2), 337–355, (2000).

[11] Lee, F. C. and Chen, W. H. On the acoustic absorption of multi-layer absorbers with different inner structures, *J. Sound Vib.*, **259**(4), 761–777, (2003).

[12] Lee, D. H. and Kwon, Y. P. Estimation of the absorption performance of multiple layer perforated panel systems by transfer matrix method, *J. Sound Vib.*, **278**(4-5), 847–860, (2004).

[13] Allard, J. F. Propagation of sound in porous media: Modelling sound absorbing materials, *Elsevier Applied Science*, London, (1993).

[14] Atalla, N. and Sgard, F. Modeling of perforated plates and screens using rigid frame porous models, *J. Sound Vib.*, **303**(1-2), 195–208, (2007).

[15] Kino, N., Ueno, T., Suzuki, Y. and Makino, H. Investigation of non-acoustical parameters of compressed melamine foam materials, *Appl. Acoust.*, **70**(4), 595–604, (2009).

[16] ISO 10534-2. Determination of sound absorption coefficient and impedance in impedance tubes -part 2: trasnfer function method. International Organisation for Standardization, Case postale 56, Geneve 20, (1998).

[17] ASTM C522, Standard Test Method for Airflow Resistance of Acoustical Materials, (2003).

[18] Ballagh, K.O. Acoustical properties of wool, *Appl. Acoust.*, **48**(2), 101–120, (1996).

[19] Kino, N. and Ueno, T. Improvements to the JohnsonAllard model for rigid-framed fibrous materials, *Appl. Acoust.*, **68**(11-12), 1468–1484, (2007).

[20] Sgard, F. C., Olny, X., Atalla, N. and Castel, F. On the use of perforations to improve the sound absorption of porous materials, *Appl. Acoust.*, **66**(6), 625–651, (2005).